Structure−Property Relationships for Electron−Vibrational Coupling in Conjugated Organic Oligomeric Systems

Luke O'Neill* and Hugh J. Byrne

FOCAS Institute and School of Physics, Dublin Institute of Technology, Kevin Street, Dublin 8, Ireland

Received: January 4, 2005; In Final Form: April 12, 2005

A series of π-conjugated oligomers containing one to six monomer units were studied by absorption and photoluminescence spectroscopy. As is common for these systems, a linear relationship between the positioning of the lowest-energy absorption and the highest-energy photoluminescence maxima plotted versus inverse conjugation length is observed, in good agreement with a simple nearly free electron model, one of the earliest descriptions of the properties of one-dimensional organic molecules. It was observed that the Stokes shift and therefore Huang−Rhys factor also exhibit a well-defined relationship with increasing conjugation length, implying a correlation between the electron−vibrational coupling and chain length. This correlation is further examined using Raman spectroscopy, whereby the integrated relative Raman scattering is seen to behave superlinearly with chain length. The Stokes shift and the Raman activity are also well-correlated in these systems. There is a clear indication that the vibrational activity and thus nonradiative decay processes are controllable through molecular structure.

Introduction

Conjugated monomeric and polymeric materials have attracted significant attention over the past few decades due to their potential applications in a range of technological areas. Organic dyes are well-established in laser applications,[1] organic molecules and polymers have long been vaunted as candidates for nonlinear optical devices,[2,3] and in the past decade, the observation of electroluminescence and stimulated emission from polymeric thin films has rejuvenated interest in this class of materials.[4,5]

Low cost and ready processability of these materials are often cited advantages, but potentially the greatest bonus is that the optical and electronic properties can be chemically tuned over a broad range. In addition to the practical advantages, this tunability enables structure−property relationships to be derived to aid material optimization as well as a fundamental understanding of the underlying physical processes in these materials.

To this end, systematic studies of oligomeric series have contributed greatly. Although they may break down in the infinite-chain-length limit of polymeric systems, simple models may be applied to such molecular series to demonstrate the effect of the π-delocalization on the optical band gap[6] and even the nonlinear optical response.[7] However, while the energetics associated with the molecular electronic structures has received considerable attention, little has been paid to the vibrational coupling processes, which compete with radiative relaxation and ultimately limit luminescence efficiencies. Extended conjugated systems are well-known for the correlation between electron and vibrational degrees of freedom,[8] and this indicates that the vibrational relationships can be defined in terms of structural variations. Several studies have been undertaken to examine vibrational−structural relationships in oligomers, from both a theoretical and an experimental viewpoint.[9,10] This study presents an investigation into the effect of oligomeric structure on easily measurable spectroscopic parameters examined through means of optical and vibrational spectroscopy, which will help to establish empirical relationships from which insight into design characteristics can be achieved. The study is aimed at developing a further understanding of the nonradiative decay processes in these materials and their structural dependence.

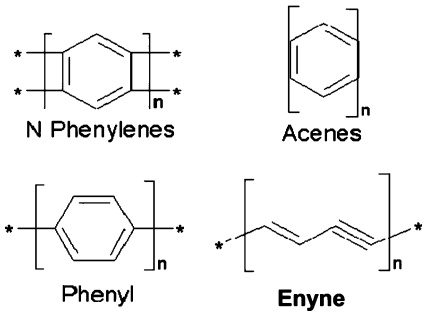

Figure 1. Structures of the *N*-phenylene, acene, phenyl, and enyne oligomer series.

The acene and phenyl oligomers, shown in Figure 1, are used to provide insight into the effect of increasing conjugation length on the photophysical properties, particularly electron−vibrational coupling, of organic materials. Results are compared to those of other related oligomeric series where available from literature, particularly the *N*-phenylenes[11] and enyne oligomers[2] shown in Figure 1. Optical absorption and photoluminescence spectroscopies are used to elucidate the electronic behavior, and Raman spectroscopy coupled with the Stokes shift are used as a probe of the vibrational coupling.

Experimental Section

The acene and phenyl series were purchased commercially. The oligomers were prepared in a chloroform solution of molarity $\sim 10^{-5}$ for the absorption and luminescence spectroscopies. Self-absorption and aggregation effects were minimized with the use of low concentrations.[12] These solutions were

* Author to whom correspondence should be addressed. E-mail: luke.oneill@dit.ie.

10.1021/jp050039w CCC: $30.25
Published on Web 06/15/2005

sonicated for 15 min to aid solubilization. The absorption spectroscopy was carried out using a Perkin-Elmer Lambda 900 UV−vis−near-IR absorption spectrometer. The luminescence measurements were performed using a Perkin-Elmer LS55 luminescence spectrometer. The other oligomeric data shown was taken from the literature and is used in a mainly comparative nature.

Raman spectroscopy was performed using an Instruments SA Labram 1B confocal Raman imaging microscope system. A helium−neon (632.8 nm/11 mW) light source was used. The light is imaged to a diffraction-limited spot via the objective of an Olympus BX40 microscope. All experiments were carried out at room temperature (300 K). For the Raman spectroscopy, the same oligomers were used but prepared as thin films of thickness ~0.5 mm by compression of the powder. A number of studies have shown that there is a negligible difference between solution and solid-state Raman spectra in similar systems, as they are dominated by the intramolecular vibrations of the polarizable π-conjugated backbone and intermolecular modes are low-energy and at most weakly coupled to the electronic system.[13−15] A 10× objective was used to maximize the focal depth and so sample the bulk of the film. The focal depth of the system was calculated to be 0.183 mm, over 100 times greater than that achieved with a 100× objective. This and the large spot size (~10 μm) helped to eliminate the effects of any slight variation in sample density. The conditions were identical for all samples, and spectral intensities were reproducible within 1%. The measurement does not enable the calculation of absolute Raman cross sections, but the reproducibility allows a semiquantitative comparative study.

Results and Discussion

In Figure 2a, the absorbance spectra of the phenyl series are shown for example. It is evident that with increased conjugation there is a considerable bathochromatic shift, as predicted by Kuhn et al.[16] Biphenyl has an absorption shoulder at 270 nm; however, by the time the series reaches a six-ringed structure (sexiphenyl), the longest wavelength absorption peak has shifted to 380 nm. By addition of four phenyl monomer units, the band gap has reduced by 110 nm (1.32 eV). The vibronic substructure also becomes increasingly evident as the chain length is increased. The presence of vibronic substructure in the absorption spectra suggests a planar rigid molecule, and there is a marked increase in the prominence of the vibronic structure as the oligomers go from the relatively flexible phenyl to the more rigid planar acene series.[17]

In the free-electron model first described by Kuhn for carbocyanine dyes[18] and adapted by Rustagi and Ducuing,[3] the dependence of the optical band gap on the conjugation length is given by

$$\Delta E = V_0 + \left(\frac{h2}{4mL_0 2} - \frac{V_0}{4}\right)\frac{1}{N+\sigma} \qquad (1)$$

where h is Planck's constant, m is the electron mass, V_0 is the infinite-chain-length band gap, L_0 is the average length of one conjugation, and N is the number of electrons in the one-dimensional box of length L, σ accounting for end-group terminations. This model predicts a systematic decrease in the band separation with increasing conjugation and has been shown to fit well with the observed behavior of the length dependence of the absorption gap for enyne oligomers.[2]

Figure 2b shows a plot of the energies of the first absorption maxima of the various oligomeric series plotted against inverse

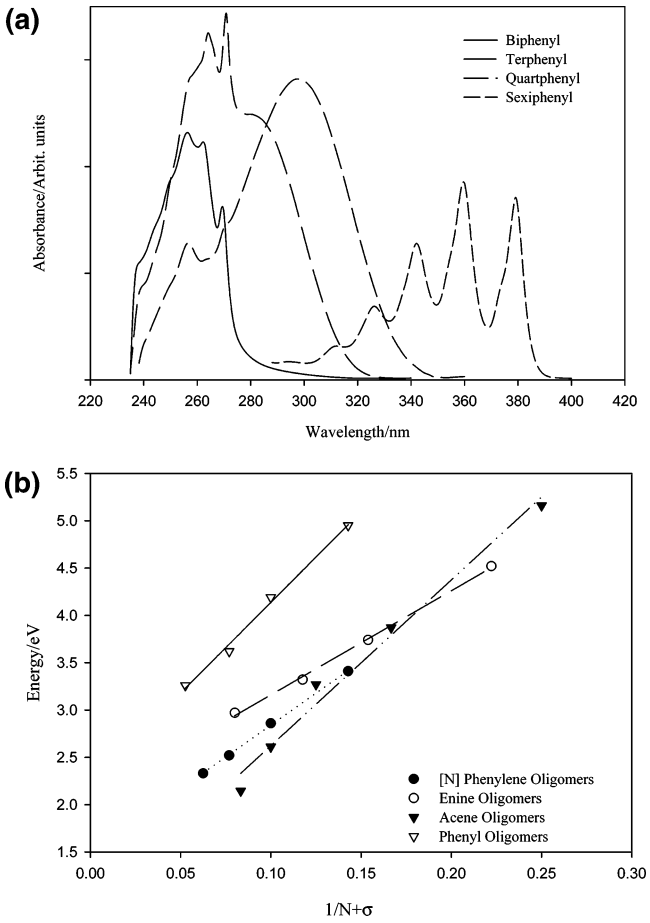

Figure 2. (a) Position of maximum absorbance versus $1/(N + \sigma)$. (b) Progression of phenyl oligomers from two to six units.

conjugation length. Along with the acene and phenyl series mentioned earlier, enyne[2] and *N*-phenylene[11] oligomers are also presented. For all series, σ is taken to be zero, as they are terminated by a C−H unit, except the enyne series for which σ is taken to be 0.5, as they are terminated by a CH_3 group.[2] For the aromatic oligomers, N is taken to be the total number of double bonds in the molecule, e.g., for naphthalene $N = 6$ and for biphenyl $N = 7$.

In all of the oligomer series, the variation in both the absorption and the emission band gap with increasing conjugation fits well to a simple nearly free electron model. Such well-defined behavior is well-established and is the basis for our understanding of linear conjugated systems.[2,19−22] It is clear, however, that both the short chain limit and the rate of decrease with increasing chain limit differ significantly with monomeric structure and the degree of coupling between the monomeric units. The differences in the long chain limit of the phenyl versus the acenes series mirrors the differences in band gaps of cis versus trans polyacetylene[7] and zigzag versus armchair single-walled carbon nanotubes.[23] In extrapolation to the infinite-chain-length limit, questions have been raised as to the role of electron−vibrational coupling. Polarons, bipolarons, and self-trapped excitons have all been reported in polymeric systems, and the debate continues over the chain length at which excited states are no longer distributed over the molecule continues.[24,25] That the oligomer series are well-behaved according to this simple model indicates that excited states are distributed over the extent of the oligomer and are thus molecular in nature. Electron−phonon quasi-particles such as polarons and bipolarons are dispersive and thus become localized on the backbone

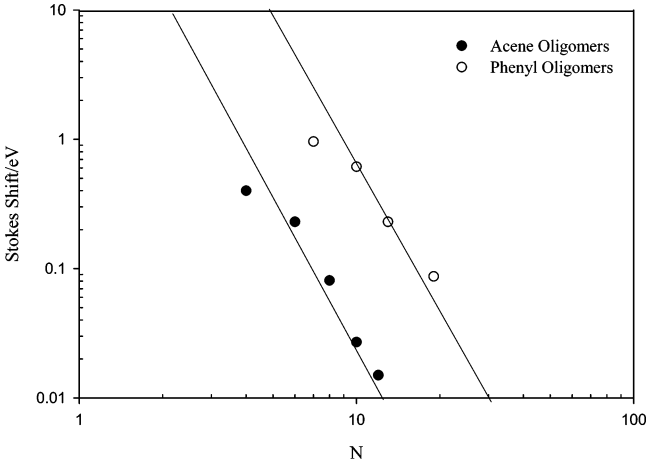

Figure 3. Stokes shift plotted versus *N*. Solid lines show a slope of −4.

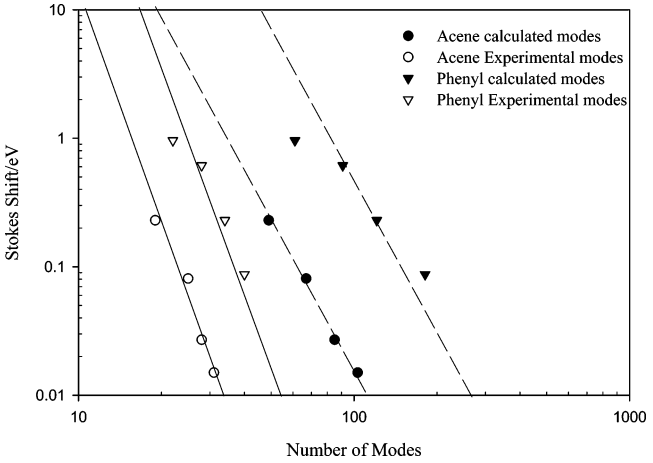

Figure 4. Stokes shift plotted versus number of modes. Solid lines show slopes of −6, and dashed line a slope of −4.

in extended systems. Such localization would limit the effective conjugation to lengths less than the molecular length. As well as introducing controversy over the nature of the excited species in these systems,[26,27] electron−vibrational coupling plays a dominant role in determining nonradiative processes. To optimize radiative relaxation in these systems, design principles to control the nonradiative relaxation of excited species are desirable. Such principles can be guided by studies of oligomeric series.

Electron−vibrational coupling is manifest in electronic spectroscopy as the Stokes shift, a result of nuclear redistribution after an electronic excitation (or relaxation).

Figure 3 shows the Stokes Shift, as calculated by the difference in the absorption and emission energy of the lowest/highest-energy transition peak for the acene and phenyl oligomer series, as a function of *N*. Presented values compare well with literature values.[17] The graph is important, as it contains information on both the electronic and the vibrational characteristics of the oligomer systems. The best fit is to a power law dependence, of order approximately −4, of the Stokes shift on the conjugation, *N*. The power dependence is similar for the phenyl and acene series and can be explained using the particle in a one-dimensional square well embedded in an elastic continuum model described by Henderson and Imbusch,[28] extended to a many-electron system as described, for example, by Kuhn.[18] Neglecting the periodic potential of eq 1, the ground-state energy can be described by

$$E_g = \frac{h2}{8m(2L)^2}N \tag{2}$$

In the excited-state energy, the dimensions of the box expand to accommodate the change in electronic configuration such that

$$E_e = \frac{h^2}{8m(2L+dx)^2}(N+1) + \frac{1}{2}kx^2$$
$$= E_e^\circ + \frac{1}{2}k\left(x - \frac{\Delta}{k}\right)^2 - \frac{\Delta^2}{2k} \tag{3}$$

where E_e° is the nonexpanded excited-state configuration and $^1/_2kx^2$ is a result of a harmonic restoring force. The system now oscillates harmonically about coordinates described by $x = \Delta/k$, and the electronic energy is reduced as a result of the excited-state reconfiguration by an amount $\Delta^2/2k$, where $\Delta = 3h^2(N+2)/8mL^3$. This energy reduction corresponds to the Stokes shift. Given that $L = L_0N$, Δ has a dominant $1/N^2$ dependence, and thus the Stokes shift has a $1/N^4$ dependence.

The simple formalism above adequately predicts the observed power law dependence in the acene and phenyl series. It ignores the periodic potential of eq 1 and also assumes that the Stokes shift is purely electronic in origin, with no contributions from relaxation of the solvent cage.[29] It furthermore assumes that the single-particle excitation is distributed over the entire molecule. The reasonable fit to the fourth-order power dependence for these shorter chain molecules gives justification for this.

The dependency of the Huang−Rhys factor (*S*), linearly dependent on the Stokes shift,[28] on the number of atoms present has been empirically described by Yu et al, as,[10] $S = a \exp(-n^2/b)$ where *a* and *b* are arbitrary constants and *n* is the number of atoms in the molecular system. This shows that *S* decreases exponentially with increasing chain length, and by extension the Stokes shift should show an exponential dependence with an increasing number of atoms. As can be seen from Figure 3, at short chain lengths there is a deviation from the fourth-order power dependence. This variation can be reconciled with the use of exponential decay, but in turn this then fails to accurately account for the Stokes shift variation at large chain lengths. The power dependence accounts more accurately for the longer-chain-length oligomers and as such will be more useful in potential application to polymeric systems.

The efficiency of the coupling to the vibrational manifold will depend on the number of modes available, *M*, which increases with chain length according to $3n - 5$ in a linear system. Thus, a fourth-order power law dependence would be expected by extrapolation of the Stokes shift dependence on length. A plot of the Stokes shift versus the calculated number of modes displays a fourth-order power law dependence. It should be noted that this dependence is only observed by including all vibrational modes of the system and not just those of the carbon framework. Although all modes will not couple equally to the electronic excitation, the role of the C−H vibrational modes in the determination of the nonradiative decay rate has been demonstrated in deuterated systems whereby an increase of the radiationless transition rates without effect on the band gap is affected.[30] Figure 4 further demonstrates the intrinsic link between the Stokes shift and the electron−phonon coupling in these systems. In general, there is a trend of decreasing Stokes shift with an increasing number of modes. The increased number of modes adds to the capacity of the molecule to distribute the excess energy. The excess energy per mode and thus the nuclear redistribution are diminished,

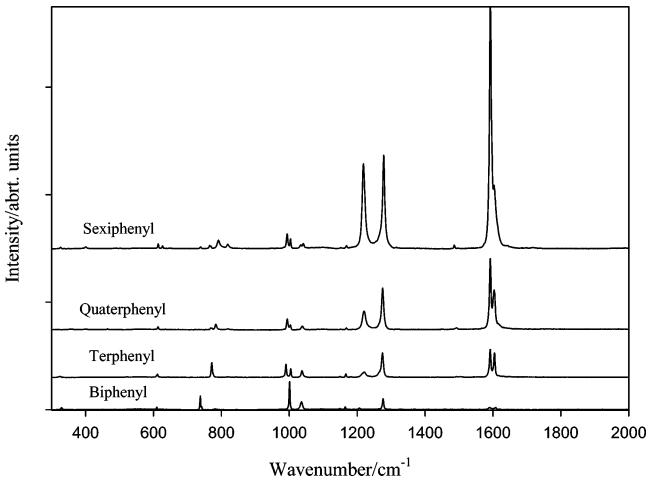

Figure 5. Plot of the Raman spectra of the phenyl oligomers. Spectra are offset for clarity.

reducing the Stokes shift. It should be noted that the Stokes shift for the phenyl series is substantially higher than that for the acene series, although the number of available vibronic modes is similar. Indeed the phenyl series has considerably more degrees of freedom in the form of rotations about the C−C ring-coupling bond. It must be concluded that it is this rotational freedom that inhibits the electron−vibrational coupling along the chain. Torsional freedom also hinders the coherence of the π-cloud disrupting the full electronic conjugation.[31] The poor fit to the fourth-order power dependence in the case of the phenyl series may be a further manifestation of this rotational freedom.

The Stokes shift is a crude measure of the electron−phonon coupling and has been shown to be dependent on temperature and sample morphology.[32,33] A more detailed approach by, for example, analysis of the Franck−Condon progressions in absorption and emission spectra is required for a full picture of how the modes couple to the electronic transitions.[34,35] It is clear, however, that the variation in this easily determinable parameter according to the oligomer chain length is well-defined. Vibrational spectroscopy,in particular Raman spectroscopy, is a direct probe of the electron−vibrational coupling and may be utilized to further illustrate well-defined relationships in these systems. Raman spectroscopy is particularly sensitive to the polarizable π-conjugated backbone, making it ideal for the (semi)quantitative analysis of the variation of electron−vibrational coupling as the oligomeric chain is modified by length or backbone structure. Raman spectra were taken in the range 100−3500 cm^{-1}. The source wavelength is far from the absorption of the samples measured, and as such the spectra may be considered nonresonant. It has however been shown that the spectral signatures of conjugated systems show negligible variation in frequency and relative intensity over a wide range of excitation wavelengths, (325−1064 nm).[36,37,13] This invariance reflects the unique coupling to the π-electronic system of all of the main modes, regardless of excitation wavelength. This is particularly so in the acene and phenyl series, with the absence of side chains or nonconjugated pendant groups.

Figure 5 shows the variation in the Raman spectrum with increasing chain length for the phenyl oligomers. It is noticeable that there is very little spectral softening as the chain length is increased. However, a significant increase in the intensity of the prominent vibrational modes is observed. The acene oligomers show a similar intensity increase but not to the same extent. The acene topology does not favor electron−vibrational coupling, and therefore the Raman intensity should be lower than that of the corresponding phenyl oligomer.[13]

Aromatic compounds are characterized by a weak C−H stretching band near 3000 $cm^{-1}$and by bands near 900−1000 and 1500−1600 cm^{-1}, which are ring breathing and stretching, respectively. The 1600 cm^{-1} band can be seen to be the most obviously varying with increasing molecular length, as would be expected as these are the frequencies corresponding to the ring structures. The other ring-associated band occurs at 1200 cm^{-1} for para-substituted benzene derivatives and can again be seen to increase systematically as the molecular length is increased. The one other significant band is at 1300 cm^{-1}, which corresponds to the C═C bond stretch that links the phenyl units, and this shows similar length dependence. Most of the other bands observed are weak overtones of other bands and of little use in the identification or characterization of the compound in question.

In Figure 4, the Stokes shift is also plotted against the number of vibrational modes observed in the Raman spectrum. The threshold for legitimate modes was set to an intensity of ≥4% of the intensity of the highest peak to avoid counting noise or other background fluctuations. While the number of accessible vibrational modes is determined by the number of degrees of freedom of the molecule ($3n - 5$), the number of Raman-active modes is determined by the molecular symmetry. This experimental determination of the number of modes underestimates the number of Raman-active modes, as many modes can be degenerate or quasi-degenerate and some may be so weak as to lie below the detection threshold of the measurement. In both cases, higher resolution and sensitivity would improve the measurement, and as such the underestimation is not a limitation of Raman spectroscopy. It should be considered, however, that it is the modes of significant intensity that represent strong electron−phonon coupling and thus are good channels for nonradiative relaxation of the excited state. This underestimation increases the observed power law dependence to the sixth order. The graph does however clearly indicate a correlation between the experimentally observable Stokes shift and Raman spectral features.

An extension of the free-electron model to Raman activity in these systems is not trivial. Theoretical studies, based on nodal analysis combined with ab initio calculations, predict a N^4 dependence of the Raman intensity for the C═C stretch of polyene systems.[10] A novel approach to the spectroscopic determination of nonlinear optical properties of conjugated materials has demonstrated that Raman cross sections can be utilized to determine the third-order hyperpolarizability of centrosymmetric conjugated molecules,[13] a parameter that has been shown to vary with a L^4 power dependence.[38] In previous studies, the dependence of the intensity of specific peaks of the Raman spectra of polyene oligomers has been seen to show a length dependence of the order $N^{2.7}$.[7] In Figure 6a, the spectrally integrated Raman intensities, in the range 100−3500 cm^{-1}, are plotted as a function of the chain length N. Intensities above 4% of the spectral maximum were numerically integrated to avoid summing background noise. Thus, the integration was taken to include the doublet in the ring-stretching modes at ∼1600 cm^{-1}. All integrated Raman intensities were normalized for molecular weight so as to give a true reflection of the variation of the intensity with increasing molecular length. The graph yields an approximate second-order power law relationship for both the phenyl and the acene systems. For the acene and phenyl series, a plot of the dominant vinyl stretch in the region of 1550−1650 cm^{-1} versus N exhibits higher-order

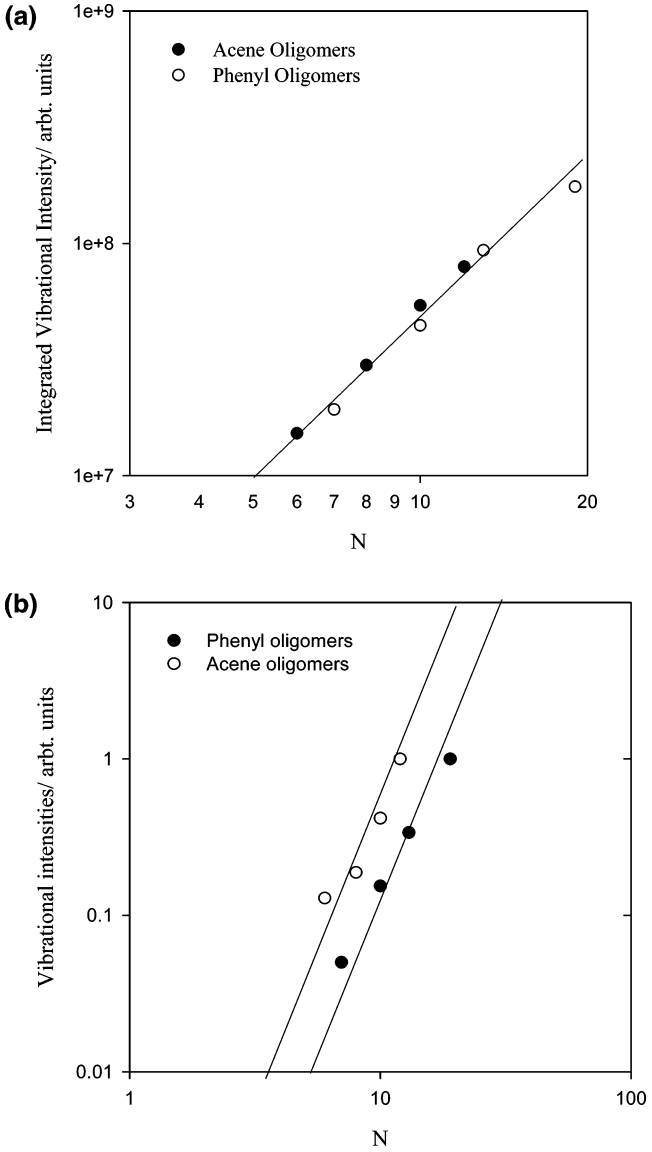

Figure 6. (a) Integrated Raman intensity plotted versus *N* integrated from 100 to 3200 cm^{-1}. (b) Relative intensities of the C═C vibrational modes along the backbone. The solid lines show slopes of (a) 2 and (b) 4.

dependence, approaching 4, as shown in Figure 6b. The conjugated C═C stretch is the most strongly dependent on the conjugation length, and integrating over the entire Raman spectrum reduces the observed power law dependence. In either representation, the spectroscopic data is well-behaved in terms of the structural variation, indicating that the electron−vibrational coupling may be characterized through routine spectroscopic investigations. Although the total number of modes is underestimated, the strength of the dominant modes, individually or integrated, is a good indication of the structural dependence of the electron correlation in these systems.

It is notable that, in contrast to the behavior for the Stokes shift, the integrated Raman intensity and the variation with conjugation are almost identical for the two sets of oligomers. The Raman activity has its primary origin in the collective normal modes of vibration but also has intensity generated from localized vibrations. The Stokes shift relies solely on the distribution of excess energy along the extent of conjugation of the molecule. Thus, the integrated Raman intensity is less affected by the rotational freedom of each of the rings in the phenyl series as it maintains the intensity localized on the rings,

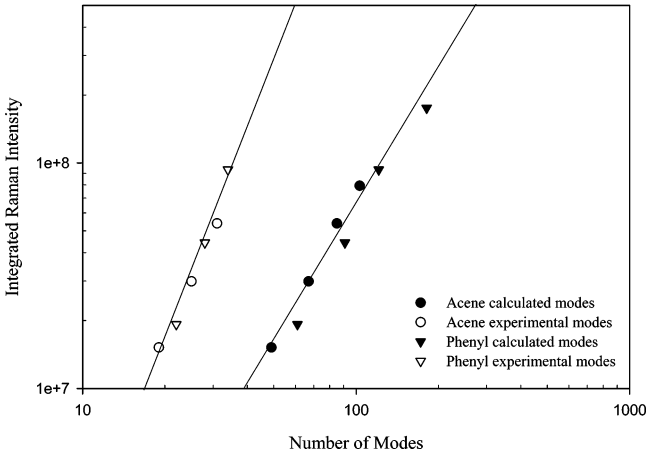

Figure 7. Integrated Raman intensity plotted versus the number of vibration modes. Solid lines show slopes of 3 (experimental modes) and 2 (calculated modes).

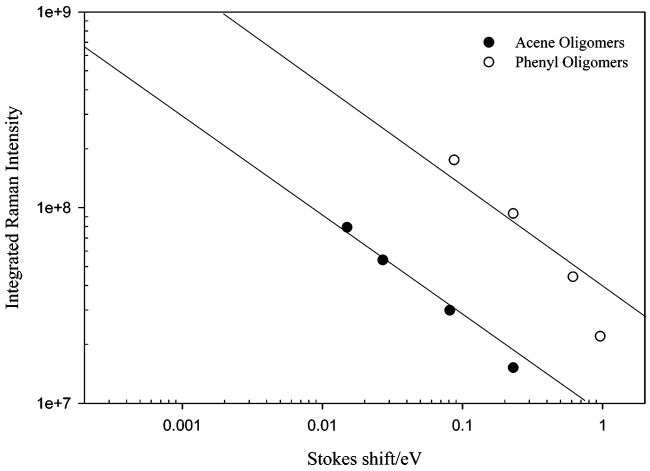

Figure 8. Plot of integrated Raman intensity versus Stokes shift. Solid lines show slopes of −0.5.

whereas this freedom significantly increases the Stokes shift in the case of the phenyl series by disrupting the distribution of the energy. The conjugated C═C stretch is consequently substantially lower in the phenyl series than in the acene series, for equivalent conjugation length.

Figure 7 shows the variation of vibrational intensity with the number of vibrational modes both experimentally observable and calculated. Again both series are seen to lie along the same trend line, and the number of available modes is underestimated by the experimental data. This is reflected again in the higher-order power law dependence of the trend for the experimental data. In comparison to the dependence of the Stokes shift on number of modes, the square dependence evident for the experimentally observable modes and the higher-order, cubic dependence observable for the calculated modes imply a square-root dependence of the integrated Raman intensity on the Stokes shift. Figure 8 illustrates that this is indeed the case, clearly at least for the acene series. The steeper behavior of the phenyl series has its origin in the deviation of the dependence of the Stokes shift on *N* from N^4 (Figure 3), attributable to the rotational freedom in this series. The Stokes shift is primarily determined by the number of modes available. The degree of electronic coupling along the chain will limit the number of modes available for distribution of the excess energy; hence any disruption in the conjugation will detrimentally affect the number of modes. The vibrational intensity per mode is also

highly dependent on the backbone conjugation, and the integrated intensity is dependent on the number of modes available. In the case of the rigid acene series, the conjugation is undisrupted, and hence all modes are available for both Raman activity and Stokes shift. However, in the case of the phenyl series, the torsional freedom disrupts the conjugation, limiting the number of available modes.

Historically, the free-electron model has been proven to be a useful tool in describing the structural dependence of the electronic properties of conjugated oligomeric series. In this study, it is extended to describe the Stokes shift, demonstrating that the electron−vibrational coupling is similarly well-behaved with backbone structure. Although the model is not extended to Raman activity, the structural dependence predicted by a more complex theoretical approach based on nodal analysis combined with ab initio calculations is demonstrated experimentally, and this behavior is empirically correlated with the structural dependence of the Stokes shift, as predicted by the free-electron model. Both the Stokes shift and the integrated Raman intensity are shown to be well-correlated measures of the electron−vibrational coupling in the oligomer. Furthermore, differences between the behavior of the two oligomer series are relatable to the molecular structure.

Conclusions

The results above demonstrate that the electron−vibrational coupling for the oligomeric systems examined do indeed behave in a well-defined manner with increased conjugation length. The Stokes shift can be correlated with the chain length and number of calculated and observable vibrational modes. Although the experimentally observed number of Raman-active modes is underestimated, the integrated vibrational activity can be correlated with the chain length. It is thus assumed that only modes of significant intensity will contribute to nonradiative relaxation processes in the excited state and therefore provide good channels for vibrational decay. By extension, it has been shown that the Stokes shift and the vibrational activity are directly related. Furthermore, the results can be understood according to a simple free-electron model as applied to the structure−property relationships of the electronic properties of oligomers. Although this is not an all-encompassing vibrational study as it only takes into account Raman spectroscopic data, the relationships found can be extended to provide a basis for a universal study of vibrational intensity variation with conjugation and thus establish universal relationships though the mutual exclusivity of Raman and IR spectroscopy. The study implies that the electron−vibrational properties of these systems and more complex polymeric systems can be tailored in a similar way to their electronic properties, pointing toward an additional route to optimization of radiative processes, by minimization of the competing nonradiative processes. The study further demonstrates that the nonradiative processes can be monitored through relatively routine spectroscopic techniques.

Acknowledgment. The FOCAS Institute is funded under the National Development Plan 2000−2006 with assistance from the European Regional Development Fund. L.O. acknowledges DIT scholarship support.

References and Notes

(1) Burroughes, J. H.; Bradley, D. D. C.; Brown, A. R.; Marks, R. N.; Mackay, K. D.; Friend, R. H.; Burns, P. L.; Holmes, A. B. *Nature* **1990**, *347*, 539.

(2) Sauteret, C.; Hermann, J. P.; Frey, R.; Pradere, F.; Ducuing, J.; Baughman, R. H.; Chance, R. R. *Phys. Rev. Lett.* **1976**, *36*, 956.

(3) Rustagi; Ducuing, K. C. *Opt. Commun.* **1974**, *10*, 258−261.

(4) Friend, R. H.; Gymer, R. W.; Holmes, A. B.; Burroughes, J. H.; Marks, R. N.; Taliani, C.; Bradley, D. C. C.; Dos Santos, D. A.; Logdlund, M.; Salaneck, W. R. *Nature* **1999**, *397*, 121−128.

(5) Wegmann, G.; Giessen, H.; Greiner, A.; Mahrt, R. F. *Phys. Rev. B* **1998**, *57*, R4218.

(6) Wenz, G.; Muller, M. A.; Schmidt, M.; Wagner, G. *Macromolecules* **1984**, *17*, 837−850.

(7) Del Zoppo, M.; Castiglioni, C.; Zuliani, P.; Zerbi, G. In *Handbook of Conducting Polymers*, 2nd ed.; Skotheim, T. A., Elsenbaumer, R. L., Reynolds, J. R., Eds.; Marcel Dekker: New York, 1998; pp 765−822.

(8) Karabunarliev, S.; Bittner, E. R.; Baumgarten, M. *J. Chem. Phys.* **2001**, *114*, 13.

(9) Gierschner, J.; Mack, H.-G.; Egelhaaf, H.-J.; Schweizer, S.; Doser, B.; Oelkrug, D. *Synth. Met.* **2003**, *138*, 311−315.

(10) Lee, J. Y.; Lee, S. J.; Kim, K. S. *J. Chem. Phys.* **1997**, *107*, 4112−4117.

(11) Dosle, C.; Lohannsroben, H.; Beiser, A.; Dosa, P. I.; Han, S.; Iwamoto, M.; Schiefenbaum, A.; Vollhardt, K. P. C *Phys. Chem. Chem. Phys.* **2002**, *4*, 2156−2161.

(12) Hedderman, T. G.; Keogh, S. M.; Chambers, G.; Byrne, H. J. *J. Phys. Chem. B* **2004**, *108*, 49.

(13) Rumi, M.; Zerbi, G.; Müllen, K.; Müller, G.; Rehahn, M. *J. Chem. Phys.* **1997**, *106*, 24−34.

(14) Diazcalleja, R.; Riande, E.; Roman, J. S. *J. Phys. Chem.* **1992**, *96*, 6843−6848.

(15) Tommasini, M.; Castiglioni, C.; Del Zoppo, M.; Zerbi, G. *J. Mol. Struct.* **1999**, *480*−*481*, 179−188.

(16) Kuhn, H. *Fortschr. Chem. Org. Naturst.* **1958**, *16*, 169.

(17) *Organic Molecular Photophysics*; Birks, J. B., Ed.; Wiley-Interscience: New York, London, 1973.

(18) Kuhn, H.; Försterling, H.-D. *Principles of Physical Chemistry: Understanding Molecules, Molecular Assemblies, Supramolecular Machines*; Wiley: New York, 2000.

(19) Graham, S. C.; Bradley, D. D. C.; Friend, R. *Synth. Met.* **1991**, *41*−*43*, 1277−1280.

(20) Narwark, O.; Maskers, S. C. J.; Peetz, R.; Thorn-Csanyi, E.; Bassler, H.; *Chem. Phys.* **2003**, *294*, 1−15.

(21) Woo, H. S.; Lhost, O.; Graham, S. C.; Bradley, D. D.; Friend, R. H. *Synth. Met.* **1993**, *59*, 13−28.

(22) Hutchison, G. R.; Yu-Jun, Z.; Delley, B.; Freeman, A. J.; Ratner, M. A.; Marks, T. J. *Phys. Rev. B* **2003**, *68*, 035204.

(23) Wildoer, J. W. G.; Venema, L. C.; Rinzler, A. G.; Smalley, R. E.; Dekker, C. *Nature* **1998**, *391*.

(24) Saricitici, N. S. *Molecular Exciton versus Semi Conductor Bond Model*; World Scientific Pub. Co., Inc.: Singapore, 1998.

(25) Fisher, A. J.; Hayes, W.; Wallace, D. S. *J. Phys.: Condens. Matter.* **1989**, *1*, 5567−5593.

(26) Kersting, R.; Molay, B.; Rusch, M.; Wenusch, J.; Leising, G.; Kauffmann, H. *J. Chem. Phys.* **1997**, *106*, 2850.

(27) Wang, X. H.; Mukamel, S. *Chem. Phys. Lett.* **1992**, *192*, 417.

(28) Henderson, B.; Imbusch, G. F. *Optical Spectroscopy of Inorganic Solids*; Clarendon Press: Oxford, U. K., 1989.

(29) Henderson, K.; Kretsch, K. P.; Drury, A.; Maier, S.; Davey, A. P.; Blau, W.; Byrne, H. J. *Synth. Met.* **2000**, *111*−*112*, 559−561.

(30) Pope, M.; Swenberg, C. E. *Electronic Processes in Organic Crystals and Polymers*, 2nd ed.; Oxford University Press: New York, 1999; p 792.

(31) Collison, C. J.; Treemaneekarn, V.; Oldham, W. J., Jr.; Hsu, J. H.; Rothberg, L. J. *Synth. Met.* **2001**, *119*, 515−518.

(32) Alloisio, M.; Cravino, A.; Moggio, I.; Comoretto, D.; Bernocco, S.; Cuniberti, C.; Dell'Erba, C.; Dellepiane, G. *J. Chem. Soc., Perkin Trans. 2* **2001**, 146−152.

(33) Gregg, B. A. *J. Phys. Chem.* **1996**, *100*, 852−859.

(34) Karabunarliev, S.; Bittner, E. *J. Chem. Phys.* **2001**, *114*, 13.

(35) Karabunarliev, S.; Baumgarten, M.; Bittner, E. R.; Mullen, K. *J. Chem. Phys.* **2000**, *113*, 24.

(36) Lefrant, S.; Buisson, J. P.; Eckhardt, H. *Synth. Met.* **1990**, *37*, 91−98.

(37) Somitsch, D.; Wenzl, F. P.; Kreith, J.; Pressl, M.; Kaindl, R.; Scherf, U.; Leising, G.; Knoll, P. *Synth. Met.* **2003**, *138*, 39−42.

(38) Byrne, H. J.; Blau, W.; Giesa, R.; Schulz, R. C. *Chem. Phys. Lett.* **1990**, *167*, 484−489.